ACS OMEGA

Open Access

http://pubs.acs.org/journal/acsodf

Article

Development of a Temperature-Responsive Hydrogel Incorporating PVA into NIPAAm for Controllable Drug Release in Skin Regeneration

Jae Hwan Choi,◆ Jae Seo Lee,◆ Dae Hyeok Yang,◆ Haram Nah, Sung Jun Min, Seung Yeon Lee, Ji Hye Yoo, Heung Jae Chun, Ho-Jin Moon, Young Ki Hong, Dong Nyoung Heo,* and Il Keun Kwon*

Cite This: *ACS Omega* 2023, 8, 44076−44085

Read Online

ACCESS | Metrics & More | Article Recommendations

ABSTRACT: Melanoma, a highly malignant and aggressive form of skin cancer, poses a significant global health threat, with limited treatment options and potential side effects. In this study, we developed a temperature-responsive hydrogel for skin regeneration with a controllable drug release. The hydrogel was fabricated using an interpenetrating polymer network (IPN) of *N*-isopropylacrylamide (NIPAAm) and poly(vinyl alcohol) (PVA). PVA was chosen for its adhesive properties, biocompatibility, and ability to address hydrophobicity issues associated with NIPAAm. The hydrogel was loaded with doxorubicin (DOX), an anticancer drug, for the treatment of melanoma. The NIPAAm-PVA (N−P) hydrogel demonstrated temperature-responsive behavior with a lower critical solution temperature (LCST) around 34 °C. The addition of PVA led to increased porosity and faster drug release. *In vitro* biocompatibility tests showed nontoxicity and supported cell proliferation. The N−P hydrogel exhibited effective anticancer effects on melanoma cells due to its rapid drug release behavior. This N−P hydrogel system shows great promise for controlled drug delivery and potential applications in skin regeneration and cancer treatment. Further research, including *in vivo* studies, will be essential to advance this hydrogel system toward clinical translation and impactful advancements in regenerative medicine and cancer therapeutics.

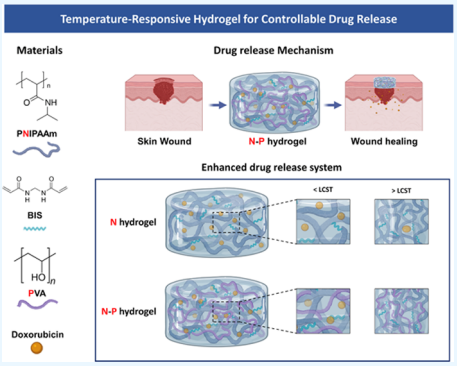

1. INTRODUCTION

Melanoma, a highly malignant and aggressive form of skin cancer originating from melanocytes, the pigment-producing cells, poses a significant global health threat with a high incidence rate.[1] It is considered the deadliest type of skin cancer primarily due to its metastatic nature, leading to a high mortality rate.[2,3] The current treatment options for melanoma, including surgery, chemotherapy, radiotherapy, immunotherapy, and targeted therapy, have inherent limitations and potential side effects.[4,5] Surgical resection, a commonly employed approach, effectively removes cancerous cells; however, it carries a high risk of tumor recurrence due to the presence of residual cancer cells at the incision site.[5,6]

In line with this, our study aims to fabricate a hydrogel-based skin regeneration medical patch to overcome the limitations of current medical patches using hydrogels.[3,7] The hydrogel was prepared using *N*-isopropylacrylamide (NIPAAm), a temperature-sensitive polymer that responds to the skin's temperature, thereby facilitating effective skin generation through controlled drug delivery.[8,9] Temperature-responsive hydrogels, which exhibit a volume phase transition at a specific temperature, have been heavily researched for drug delivery purposes and are categorized as stimuli-responsive polymers. Poly(*N*-isopropyl-acrylamide) (PNIPAAm), a representative temperature-sensitive hydrogel polymer, exhibits a Lower critical solution temperature (LCST) at 32−34 °C. Consequently, it swells at temperature below the LCST and shrinks at temperature above the LCST.[10] Those properties are advantageous for controlling drug release through hydrogel volume shrinkage at the body temperature. However, NIPAAm alone exhibits a drawback of slow response to temperature changes, which limits its applications in temperature-responsive drug delivery.[11,12] To overcome this limitation, various methods are being developed and applied. Among them, the formation of a dual network through an interpenetrating polymer network (IPN) structure has gained attention for improving the response rate to temperature changes.[12−15]

In our study, we developed a hydrogel based on the IPN. The IPN structure can be divided into semi-IPN and full-IPN.

Received: August 24, 2023
Revised: October 9, 2023
Accepted: October 30, 2023
Published: November 7, 2023

The semi-IPN consists of two or more networks that partially intertwine in a combined polymer network but do not undergo cross-linking, while the full-IPN completely intertwines the networks. Both types of IPN remain their structure integrity unless the chemical bonds are disrupted.[16] Specifically, our study focused on fabricating a semi-IPN hydrogel, where the non-cross-linked network of NIPAAm and poly(vinyl alcohol) (PVA) coexist. PVA was chosen as a useful material in drug delivery due to its high adhesive property, biocompatibility, and nontoxicity. Furthermore, the incorporation of PVA can address the issue of hydrophobicity commonly associated with PNIPAM polymers, resulting in an enhanced internal structure with increased density.[17−19] Consequently, this modification allows for precise control over the release rates of substances from the hydrogel. Moreover, we used doxorubicin (DOX), an anticancer drug, as a drug model.[20]

Consequently, our study aimed to fabricate a NIPAAm-PVA (N−P) hydrogel encapsulating DOX, enabling stable anticancer effects and promoting skin regeneration through the controlled release of additional drugs triggered by the skin's temperature response. Our ultimate goal was to develop a skin treatment medical patch that effectively delivers drugs in response to the skin's temperature. To evaluate the performance of the fabricated N−P hydrogel, we conducted chemical characterization, mechanical properties, and *in vitro* biocompatibilities, ensuring its suitability for application in a skin treatment medical patch.

2. MATERIALS AND METHODS

2.1. Materials. *N*-isopropylacrylamide (Mw: 113.16 g/mol)(NIPAAm), Poly(vinylalcohol) (M_W: 30,000−70,000 g/mol, 87−90%) (PVA), and *N*,*N*′-Methylenebis(acrylamide) (M_W: 154.17 g/mol, 99.5%) (BIS) were purchased from Sigma-Aldrich. Ammonium Peroxdisulfate (M_W: 228.19 g/mol, 99.0%) (APS), and *N*,*N*,*N*′,*N*′-Tetramethylethylenediamine (M_W: 116.21g/mol, 98%) (TEMED), were purchased from Tokyo Chemical Industry Co. Ltd. (Tokyo, Japan). Fourier Transform Infrared was used on a Cary 630 (Agilent Technologies). Differential Scanning Calorimeter was used N-650 (Scinco, Korea). Rheological rheometer was a MCR 92 (Anton Paar, Korea). Cell viability assay kit was used EZ-Cytox (Dogenbio, Korea). Spectrophotometer was a Multiskan GO (Thermo Scientific). Microscope was used with an EVOS XL Core (Invitrogen). HaCaT, human keratinocyte cell line, was purchased from Cell Lines Service (Eppelheim, Germany). Dulbecco's modified Eagle's medium (DMEM), fetal bovine serum (FBS), penicillin and streptomycin (PS), TrypLE Express, and Dulbecco's phosphate buffered saline (DPBS) were purchased from GIBCO (Grand Island, NY). Doxorubicin was purchased from Sigma-Aldrich.

2.2. Preparation of NIPAAm-PVA (N−P) hydrogels. NIPAAm (8 wt %) and PVA (4 wt %) were dissolved in distilled water, followed by mixing with BIS. The mixture was then reacted by adding APS (10 wt %) and TEMED. The polymerization and cross-linking process occurred during stirring for 17 h at 16 °C.[19] The compositions of NIPAAm-PVA (N−P) hydrogels under various conditions are indicated in Table 1.

2.3. Characterization of N−P hydrogels. The lower critical solution temperature (LSCT) of the prepared N−P hydrogel was measured by using a differential scanning calorimeter (DSC, N-650, Scinco). The hydrogel was immersed in distilled water at room temperature for 48 h to reach the equilibrium swelling state, and then it was placed in the liquid pan of the DSC and sealed. The measurement was performed with a heating rate of 2 °C/min, ranging from 25 to 40 °C. The onset of heat absorption peak in the DSC curve of the hydrogel was determined as the LCST.

Table 1. Composition of the hydrogel and manufacturing conditions

	sample codes			
compositions	N−P0	N−P1	N−P2	N−P3
NIPAAm (μL)	400	340	260	200
BIS (mg)	0.64	0.64	0.64	0.64
PVA (μL)	0	60	140	200
APS (μL)	5	5	5	5
TEMED (μL)	6	6	6	6

The cross-linking of the prepared hydrogel was confirmed using Fourier transform infrared (FT-IR) spectroscopy (Cary 630, Agilent Technologies). The wavelength ranges from 4000 to 400 cm^{-1} was measure using the attenuated total reflectance (ATR) method on the freeze-dried hydrogel samples.

The morphological structures of the lyophilized N−P hydrogel samples were observed using a scanning electron microscope (SEM, Hitachi SU8010, Japan).

To evaluate the degree of swelling, the hydrogel was fluorescently stained and images were captured at each state. The diameter of the hydrogel was quantified to compare and evaluate the degree of swelling among the hydrogels.

The degradation behavior of the N−P hydrogels was investigated by preparing 400 μL of N−P hydrogels in DPBS at 37 °C. The hydrogels were removed from the solution at predetermined time points, dried, and weighed. The degradation rate of the hydrogels was calculated as follows:

$$\text{degradation ratio}\,(\%) = \frac{W_t}{W_0} \times 100$$

Where W_t and W_0 are the initial and final weights of the hydrogels, respectively.

To investigate the rheological properties of the N−P hydrogels, we prepared hydrogels with different concentrations of PVA were prepared. The storage modulus (G') and loss modulus (G'') of each sample were measured. A frequency sweep was performed in the range of 0.1−10 Hz under a constant strain of 1%. Subsequently, the values of G' and G'' were calculated.

2.4. Cell viability and proliferation. To evaluate the cell viability of materials, 400 μL of N−P hydrogel was placed in a transwell. HaCaT cells were then seeded at a concentration of 5×10^3 cells/mL at the bottom of 24 well tissue plates. At predetermined times (24 and 48 h), live cells were treated with a mixture solution of Calcein, AM (C3100MP, Invitrogen) and Ethidium Homodimer-1 (E1169, Invitrogen) for 30 min. After washing with DPBS, the stained cells were observed by using a fluorescence microscope (EVOS M7000, Invitrogen).

To evaluate the cell proliferation of materials, 400 μL of the N−P hydrogel was placed in a transwell. HaCaT cells were seeded at a concentration of 1×10^4 cells/mL at the bottom of 24 well tissue plates. The cells were then cultured for the culture period in 24 well tissue plates. The culture medium was changed every 3 days. After 1, 3, and 7 days of culture at 37 °C in a 5% CO_2 atmosphere, 500 μL of an EZ-Cytox (Dogenbio,

https://doi.org/10.1021/acsomega.3c06291
ACS Omega 2023, 8, 44076−44085

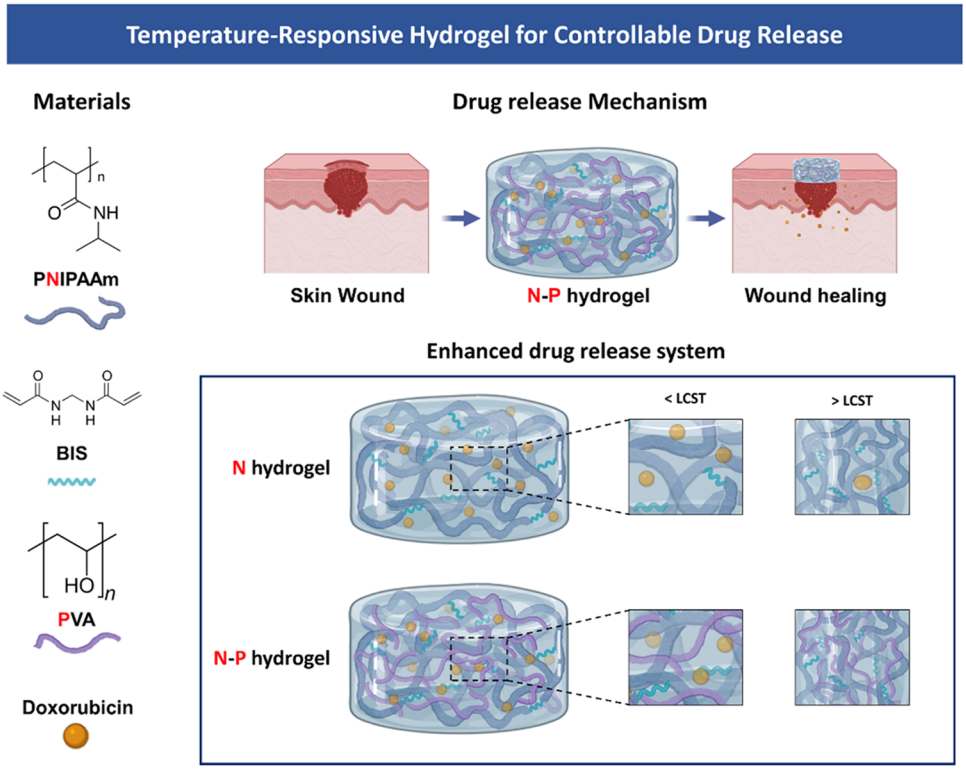

Figure 1. Schematic Illustration of the temperature-responsive N−P hydrogel.

Korea) was added to each well, and the plate was incubated for 1.5 h. The absorbance was measured at 450 nm using a Benchmark Plus microplate spectrophotometer (BR170-6930, Bio-Rad, Hercules, CA).

2.5. Release kinetics of DOX from N−P hydrogels. To evaluate the drug release of the N−P hydrogel, 400 μL hydrogel samples were prepared and subjected to freeze-drying. The freeze-dried samples were then swollen in a doxorubicin (DOX) solution at 4 °C for 3 days. The DOX solution was prepared at a concentration of 100 μg/mL by dissolving it in DPBS. After gently wiping the surface of the DOX-loaded hydrogel to remove any excess surface drugs, it was immersed in DPBS at 37 °C to initiate drug release. Samples were collected at different time points, and their absorbance was measured at 480 nm using a microplate spectrophotometer.

2.6. Evaluation of anticancer effect *in vitro*. For the evaluation of anticancer effect *in vitro*, the same drug-loaded hydrogel method was used as the drug release method, with the concentration of DOX set at 5 μg/mL. The groups compared and evaluated were the cell-only group and the group without hydrogel, where DOX was dissolved in the media at a concentration of 5 μg/mL. B16-F10 melanoma cells were cultured in a 24-well transwell plate and seeded at a density of 3×10^4 cells. After 1 and 2 days of culture at 37 °C in a 5% CO_2 atmosphere, 500 μL of an EZ-Cytox was added to each well, and the plate was incubated for 1.5 h. The absorbance was measured at 450 nm using a microplate spectrophotometer.

Additionally, to assess cell death in melanoma cells induced by drug release, we investigated alterations in cell morphology and drug penetration using a Lysotracker Green DND-26 (Invitrogen). B16-F10 cells were cultured on a coverslip and seeded at a density of 3×10^4 cells. The experimental groups followed the same protocol as that in the previous experiment. Prior to hydrogel application, the cultured cells were incubated with a concentration of 2 μM Lysotracker for 30 min. Subsequently, after washing, the culture medium was replenished, and the DOX-loaded N−P hydrogel was applied to initiate DOX release. At specific time intervals, the cells were fixed using 4% paraformaldehyde and subjected to evaluation through the acquisition of fluorescent images.

2.7. Statistical analysis. Prism 9 (GraphPad Software) was used to perform statistical analyses. All values are presented as the mean ± standard deviation. One-way analysis of variance (ANOVA) was followed by Dunnett's T_3 post hoc test to perform multiple comparisons. Differences having sufficiently low p-values ($^*p < 0.05$, $^{**}p < 0.01$, $^{***}p < 0.001$) were considered to be statistically significant.

3. RESULTS AND DISCUSSION

3.1. Fabrication and characterization of temperature responsive N−P hydrogel behavior. We selected the temperature-sensitive PNIPAM polymer as the primary component for drug release and combined it with the PVA polymer to create a hydrogel capable of facilitating drug release with ease and rapid degradation (Figure 1). Generally, the inclusion of a second polymer in the PNIPAM hydrogel network increases its hydrophilicity compared with PNIPAM alone. As a result, channels are formed during the swelling process through which water can readily diffuse, further enhancing these properties in the interpenetrating network (IPN).[18,19] To investigate the thermal characteristics of temperature-responsive N−P hydrogels, we conducted LCST measurements on the prepared hydrogels using DSC. The N−P hydrogels were subjected to temperature changes ranging from 25 to 45 °C at a rate of 2 °C/min, and the results are presented in Figure 2a. From the DSC results, it was observed

https://doi.org/10.1021/acsomega.3c06291
ACS Omega 2023, 8, 44076−44085

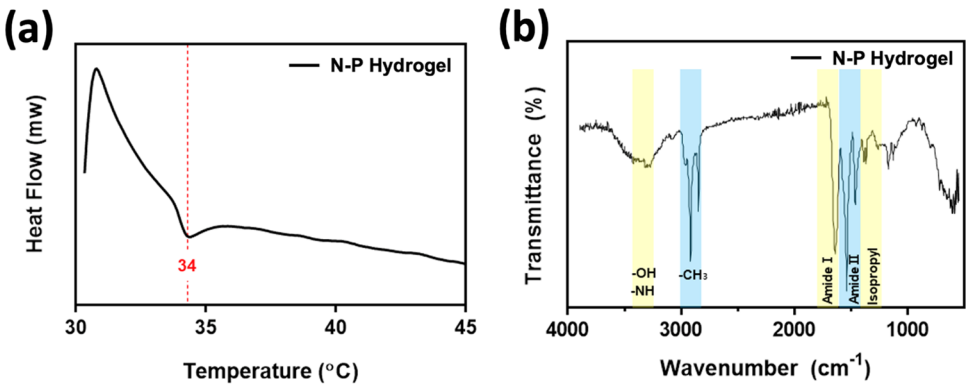

Figure 2. Characterization of N−P hydrogel: (a) DSC analysis and (b) IR analysis.

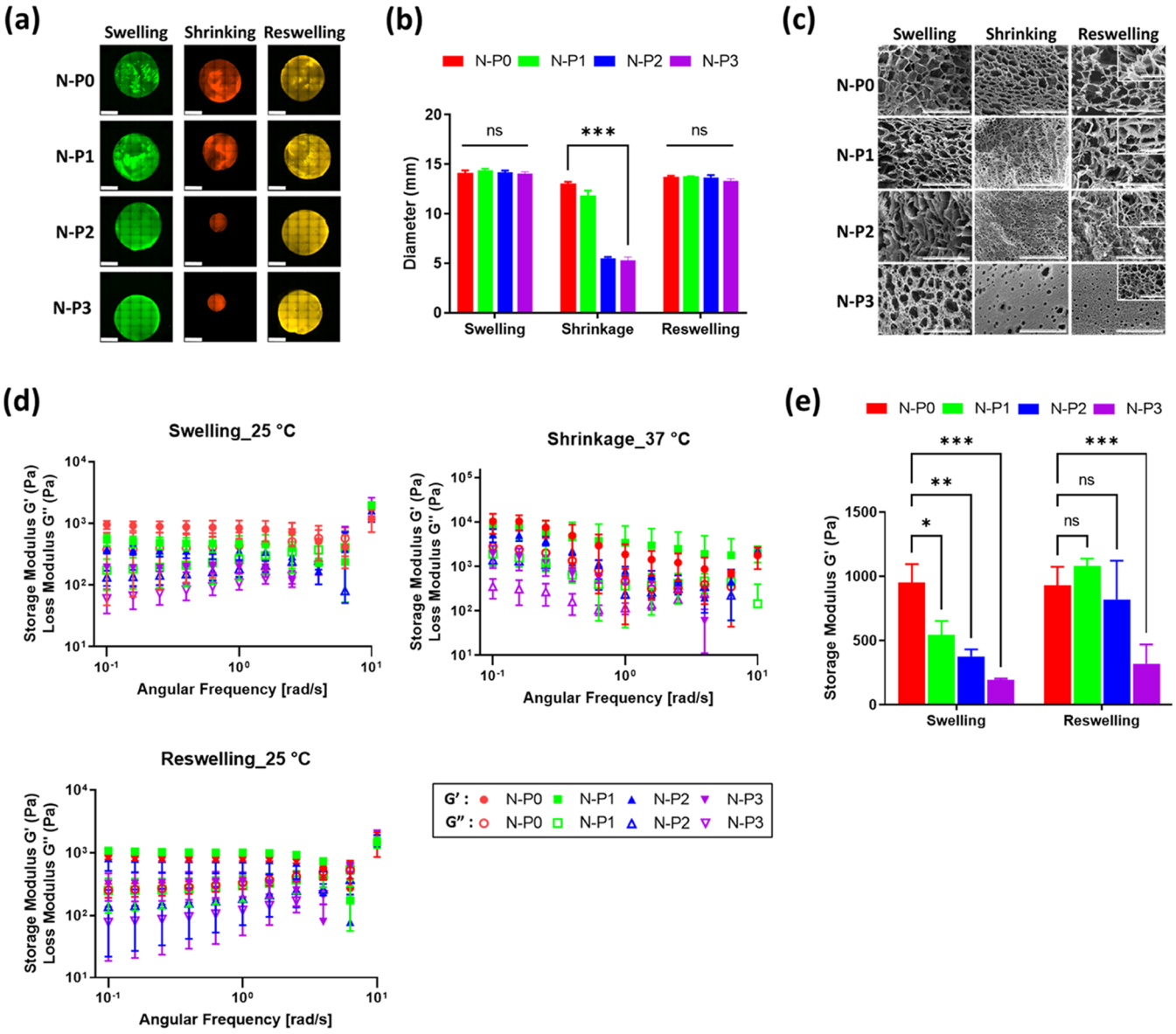

Figure 3. Evaluation of N−P hydrogel: (a) swelling ratio − representative fluorescence image (scale bar = 5 mm), (b) diameter measurement of N−P hydrogels (n = 3, ***p < 0.001), (c) SEM image (400× and 2.0k×, large scale bar = 100 μm and small scale bar = 20 μm), (d) storage and loss modulus (G' and G'') of N−P hydrogels after swelling, shrinking, and reswelling, and (e) storage modulus comparison after swelling and reswelling (n = 3, *p < 0.05; **p < 0.01; ***p < 0.001).

that all of the prepared hydrogels exhibited a distinct exothermic peak at approximately 34 °C, indicating a phase transition. This finding suggests that the LCST of the prepared hydrogels can be estimated to be around 34 °C. It is

https://doi.org/10.1021/acsomega.3c06291
ACS Omega 2023, 8, 44076−44085

noteworthy that the presence of the PNIPAAm polymer in the N−P hydrogels accounts for their LCST behavior. Consequently, below the LCST temperature, the prepared hydrogels existed in an expanded state when in contact with an aqueous solution. However, upon reaching temperatures above the LCST, a volume phase transition occurred, causing the N−P hydrogel to undergo condensation. This transition is expected to result in the release of substances from the N−P hydrogel into the surrounding environment, providing the desired effect for controlled drug delivery.[14,21] In addition, FT-IR spectroscopy was used to confirm the chemical structure of the N−P hydrogel incorporated with the two polymers. As shown in Figure 2b, the spectra of the synthesized polymer N−P exhibited distinct peaks at approximately 1658 and 1541 cm^{-1}, attributed to stretching vibrations of C = O, primary amide, and N−H bending vibrations.[22] These peaks indicate the presence of cross-linking in the PNIPAM polymer structure. Additionally, a peak at around 1458 cm^{-1} was observed, which is associated with the presence of the isopropyl group and corresponds to the $-CH_3$ vibration, $-CH_2$ scissoring, and C−N stretching vibrations. Peaks at approximately 1388 and 1369 cm^{-1} further confirm the presence of the isopropyl group, solidifying the presence of PNIPAM in the synthesized polymer structure.[22,23] The peaks at around 1373 and 2890 cm^{-1} correspond to the $-CH(CH_3)_2$ and −CH− vibrations, respectively, indicating the presence of PNIPAM.[24] The presence of PVA was confirmed by characteristic peaks at 1095, 1372, and 1143 cm^{-1}, associated with C−O−H stretching, C−H bending vibrations, and crystallization of PVA, respectively.[24,25] In this absorption region, the permeability of the hydrogel increased with an increase in the PVA content. Therefore, the FT-IR analysis confirmed the successful cross-linking of the hydrogel, as evidenced by the observed characteristic peaks and vibrations associated with the constituents of the N−P hydrogel. This temperature-dependent response of the N−P hydrogel provides a promising mechanism for precise and controllable drug delivery, particularly for skin regeneration applications.[18,24]

3.2. Physical Characterization of N−P hydrogel according to temperature. To evaluate the degree of swelling, the diameter of the hydrogels was measured to compare and assess the degree of swelling among the different hydrogel groups (Figure 3a). In the swollen state, all groups exhibited similar diameters of approximately 14 mm. However, after undergoing a 1 h contraction at 37 °C, differences in diameter were observed among the groups. In the shrunken state, the diameter of the N−P0 hydrogel decreased to 13.07 ± 0.25 mm, while N−P1 shrank to 11.86 ± 0.41 mm. N−P2 and N−P3 hydrogels exhibited contractions to 5.52 ± 0.11 mm and 5.30 ± 0.29 mm, respectively (Figure 3b). This indicated that the addition of PVA resulted in higher degrees of contraction in the hydrogel.[15,26−28] Subsequently, upon reswelling, all groups demonstrated a reswelling rate of over 94% compared with the initial swollen state. This finding confirms that the dual network introduced by the addition of PVA enhances the responsiveness and swelling ratio of the temperature-responsive N−P hydrogel. This enhancement is attained by introducing a pathway for moisture release through the addition of PVA, thereby further enhancing the reactivity of the NIPAAm hydrogels. Conventional NIPAAm hydrogels undergo a hydrophilic−hydrophobic transition at temperatures above LCST that initiates from the surface, resulting in the formation of a thicker layer during the contraction process and leading to a drawback of a reduced reaction rate. Nevertheless, the inclusion of PVA initiates the formation of the moisture release pathway, effectively addressing this limitation and augmenting the responsiveness of NIPAAm.[18,26−28] To investigate the interconnected structures, the lyophilized N−P hydrogels were observed by using SEM. SEM images were captured in the swollen, shrunken, and reswollen states. As shown in Figure 3c, it was observed that as the content of PVA increased, the size of the pores decreased consistently. Furthermore, in the case of N−P3, a formation of smaller pores within the larger macropores was observed, which is a characteristic feature of the interpenetrating polymer network (IPN) structure.[29] The pore size was found to decrease, and the porosity increased from the swollen to the shrunken state. By incorporating the PVA polymer, the hydrogel gains the ability to form an additional network through IPN, which further improves the performance of reactive hydrogel based on NIPAM. The IPN method can be employed to partially network PVA, making the inner structure becomes significantly more refined and structured.[19,27−29] However, during reswelling, only the hydrogel without PVA (N−P0) was able to fully recover the initial pore size observed in the swollen state. It was also noted that as the amount of PVA increased, the restoration of pore size upon reswelling was less effective, indicating a lower degree of pore restoration in the reswollen state. Therefore, the results obtained from the swelling evaluation, in conjunction with the SEM images, indicate that the addition of PVA in the hydrogel leads to increased porosity, which enhances the water release channels and the responsiveness of the temperature-responsive N−P hydrogel based on NIPAAm.

The rheological properties of the N−P hydrogels were evaluated to assess their characteristics. Initially, N−P hydrogels were evaluated at 25 °C after maximum swelling. As shown in Figure 3d, the highest storage modulus (G') value was observed in the N−P0 group, reaching 949.89 ± 118.66 Pa. It was observed that as the concentration of PVA increased, the rheological properties decreased. Similarly, when the N−P hydrogels were evaluated at 37 °C in the shrunken state, the N−P0 group exhibited the highest storage modulus with a value of 10,310.17 ± 4026.4 Pa. As the concentration of PVA increased, the rheological properties consistently decreased. However, after the contraction phase and entering the reswollen state, the N−P0 group showed a storage modulus value of 928.91 ± 118.5 Pa, which was similar to the initial swollen state. In contrast, the groups containing PVA demonstrated an increase in the storage modulus. This observation is consistent with the SEM analysis and suggests an increase in density associated with an increase in porosity after the contraction phase.

The behavior described above can be attributed to the temperature-responsive polymer, NIPAAm. At temperatures below the LCST, NIPAAm remains hydrophilic, absorbing water and swelling due to the formation of hydrogen bonds. However, at temperatures above the LCST, NIPAAm transitions to a hydrophobic state, leading to contraction and the release of water along with the collapse of hydrogen bonds.[8] During the reswelling phase, the hydrogels regain their hydrophilic properties, forming additional hydrogen bonds with the hydrophilic PVA network, resulting in an increase in rheological properties.[30] In summary, the rheological evaluation of the N−P hydrogels demonstrates the temperature-

https://doi.org/10.1021/acsomega.3c06291
ACS Omega 2023, 8, 44076−44085

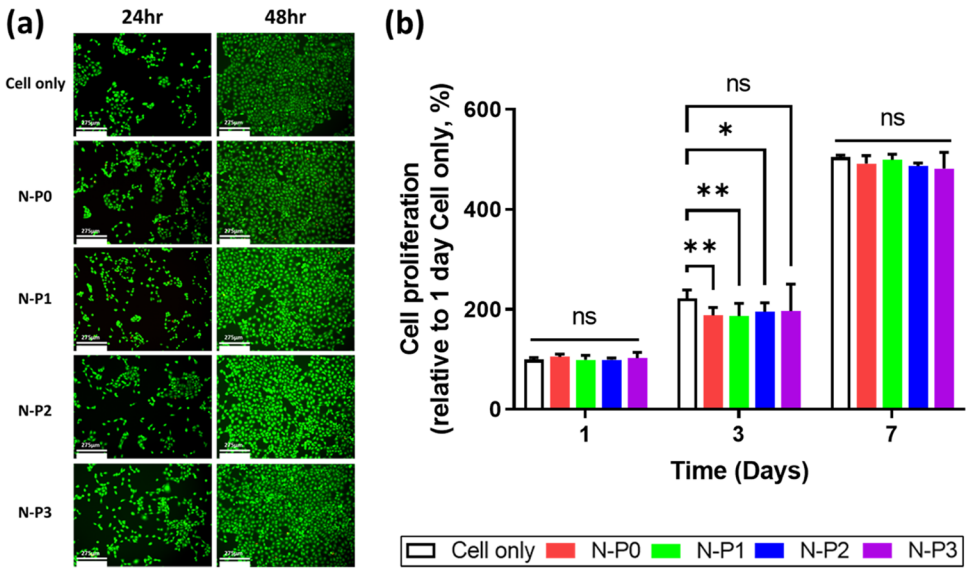

Figure 4. Evaluation of cell viability and proliferation of N−P hydrogel by transwell culture system: (a) representative LIVE/DEAD staining images of HaCat cells (scale bar = 275 μm), (b) cell proliferation rate by CCK (n = 5, *p < 0.05; **p < 0.01).

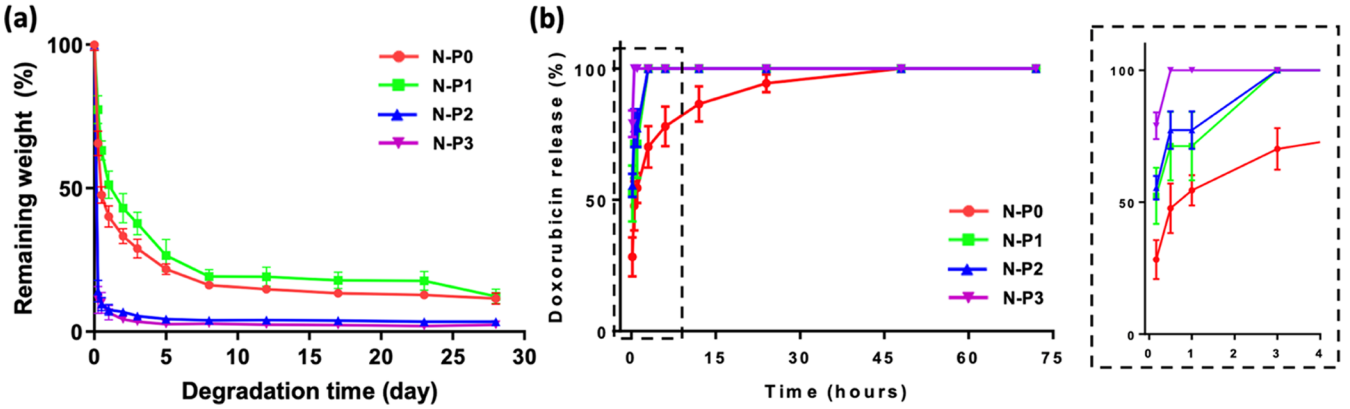

Figure 5. Evaluation of N−P hydrogels according to amount of PVA: (a) degradation behavior of N−P hydrogels (n = 5), and (b) *in vitro* DOX release kinetics from N−P hydrogels (n = 5).

responsive behavior of NIPAAm and the effect of PVA content on the rheological properties. The increase in porosity during the contraction phase contributes to enhanced density, and the subsequent reswelling leads to the formation of additional hydrogen bonds with the hydrophilic PVA network, resulting in increased rheological properties.

3.3. *In vitro* biocompatibility and cell proliferation of N−P hydrogel. To access the biocompatibility of the N−P hydrogel, cell viability and proliferation assays were conducted by using a transwell culture system. Cell viability was evaluated by using live/dead staining, and cell proliferation was assessed by using EZ-Cytox. The live/dead staining results revealed that most of the HaCaT cells appeared bright green, indicating the absence of distinct dead cells. The initial 24 h cell viability of the N−P1 group showed a relatively low value of 79%. However, at the subsequent 48 h, all groups of HaCaT showed more than 80% viability. Furthermore, all experimental groups including the control group exhibited nonspecific cell viability. These findings suggest that the presence of PVA had no significant impact on cell viability (Figure 4a). Afterward, cell proliferation evaluation was performed on days 1, 3, and 7. All experimental groups showed a cell proliferation rate of 180% or higher compared to the cell-only group on the 1st day, and this rate further increased to 480% or more on the 7th day. Nonspecific cell proliferation rates were observed in all experimental groups, including the control group. Consequently, it was confirmed that the content of PVA did not affect the cell proliferation rate (Figure 4b). Based on these results, it can be inferred that all experimental groups, including those with varying levels of PVA, demonstrated noncytotoxicity and supported cell proliferation during the initial period.[17,31] The N−P hydrogel showed excellent *in vitro* biocompatibility, providing a suitable environment for cell survival and proliferation. These findings further support the potential of the N−P hydrogel as a promising candidate for various biomedical applications including skin regeneration.

3.4. Correlation between degradation effect and drug release *in vitro*. To confirm the correlation of drug release through hydrogel degradation, the degradation behavior was conducted at 37 °C. The weight of the hydrogels was measured at various time points for comparison and evaluation. Initially, all groups exhibited contraction behavior attributed to the temperature-responsive polymer NIPAAm, rather than degradation of the hydrogels (Figure 5a). Subsequently, after completing the contraction phase, degradation of the hydrogels commenced. Notably, the N−P2 and

https://doi.org/10.1021/acsomega.3c06291
ACS Omega 2023, 8, 44076−44085

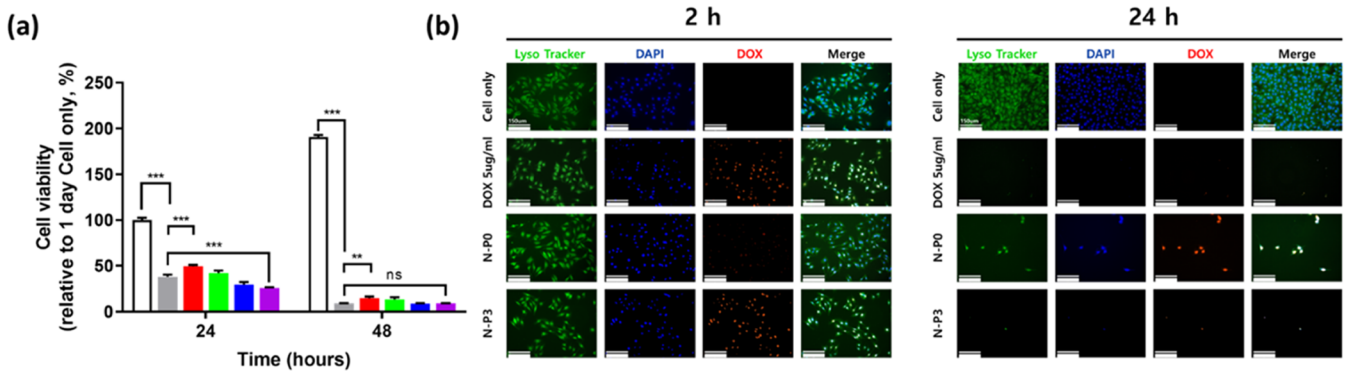

Figure 6. *In vitro* anticancer effects of the DOX loaded N−P hydrogel by transwell system: (a) cell viability rate of B16−F10 melanoma cell by CCK (n = 5, $^{**}p < 0.01$; $^{***}p < 0.001$), and (b) Fluorescence image of 2 and 24 h (scale bar = 150 μm, Endosome/lysosome and nuclei were stained with Lysotracker Green DND-26 and DAPI, respectively).

N−P3 groups exhibited rapid degradation after the initial contraction. By the 5th day and 2nd day, respectively, N−P2 and N−P3 had lost 95% of their initial weight, reaching a maximum degradation of 98% by day 28. However, the N−P0 and N−P1 groups displayed slower degradation, with 77 and 71% degradation, respectively, by the 5th day after the initial contraction. Even on day 28, they (N−P0 and N−P1) exhibited a degradation rate of 89%, indicating relatively slower degradation. These results suggest that the increased PVA content contributed to enhanced degradation, as the IPN structure resulting from the presence of PVA led to rapid contraction behavior and significant contraction ratios, resulting in accelerated degradation performance.[18,32] The results demonstrate that the degradation of the N−P hydrogels increased with a higher PVA content. The inclusion of PVA in the IPN structure not only induced rapid contraction behavior and higher contraction ratios but also led to a faster degradation performance. It is expected to result in a substantial increase in density of the internal structure, introducing PVA, enabling it to accommodate a higher drug load.

To assess the drug release behavior of the N−P hydrogel, doxorubicin (DOX) was utilized as the model drug, and the experiments were conducted at 37 °C (Figure 5b). The DOX release behavior exhibited a faster release as the PVA content increased. N−P3 released 78% of doxorubicin within 10 min and completely released all the drug within 30 min. Subsequently, N−P2, N−P1, and N−P0 exhibited the sequential completion of drug release. These findings further support the previous results, demonstrating the accelerated release with increasing PVA content.[19,27,28] The rapid drug release behavior, observed as a consequence of increased PVA content, can be attributed to mechanisms such as increased porosity leading to higher swelling ratios and lower mechanical properties.[27,29] Additionally, the subsequent increase in swelling ratio coupled with a higher contraction ratio induces faster degradation.[18,32] This accelerated drug release behavior, resulting from the combination of these mechanisms, can be attributed to the incorporation of PVA into the NIPAAm hydrogel, which forms an IPN structure.[33] Therefore, the results indicate that the addition of PVA, leading to the formation of a dual network through the IPN structure, facilitates rapid drug release in the N−P hydrogel. The enhanced drug release behavior is attributed to the increased porosity, higher swelling ratios, and greater contraction ratios associated with the PVA content. These findings highlight the potential of the N−P hydrogel as a drug delivery system for efficient and controlled drug release applications including skin regeneration. It can adapt to irregular shapes immediately after surgery and represents a promising option for skin remodeling to achieve rapid drug release.

3.5. *In vitro* anticancer Effects of the DOX-loaded N−P Hydrogel. Based on the previous results indicating rapid drug release behavior, we evaluated its impact on cell viability using DOX as the drug of interest (Figure 6a). In the media containing DOX, the cell viability at the initial 24 h showed 38.2% compared to the cell only group. The N−P0 group, which exhibited the slowest drug release, showed a 49.62% cell viability. In contrast, the N−P3 group, with the fastest drug release, displayed a cell viability of 25.82% at the same time point. After 48 h, the cell viability in the media containing DOX group was 9.1%, N−P0 showed 14.59%, and N−P3 showed 9.1% cell viability. The lower cell viability observed in the N−P3 group compared to the media containing the DOX group at the initial time point suggests that the faster drug release in N−P3 may be more effective for melanoma treatment. Additionally, we used LysoTracker to observe the morphology of B16−F10 cells in each group (Figure 6b). At the initial 2 h, the rapid drug release in N−P3 led to the complete release of DOX, penetrating the cells. The cells appeared thinner compared with the cell only group. After 24 h, both the media containing the doxorubicin group and N−P3 group showed complete cell death, while N−P0, with slower drug release, still had viable cells. In comparison to the normal B16-F10 cells with a spindlelike shape, the cells exposed to DOX exhibited thin and elongated nuclei, indicating cell apoptosis. Subsequently, the cells ultimately assumed a rounded shape, indicating complete cell death.[34] The results suggest that the rapid drug release behavior of the N−P hydrogel, particularly observed in the N−P3 group, can lead to more effective melanoma treatment. The LysoTracker observations further support the efficient drug delivery and apoptotic effect on melanoma cells induced by the N−P hydrogel, particularly in the N−P3 group. These findings highlight the potential of the N−P hydrogel as a promising candidate for anticancer drug delivery applications. However, promising the *in vitro* results may be, it is crucial to acknowledge that the translation from *in vitro* to *in vivo* settings is a complex and critical step in evaluating the potential clinical application of the N−P hydrogel. Nonetheless, a cautiously optimistic perspective regarding the in vivo feasibility of N−P hydrogels persists. This optimism is

https://doi.org/10.1021/acsomega.3c06291
ACS Omega 2023, 8, 44076−44085

grounded in the outcomes of preclinical assessments conducted within an animal model utilizing a temperature-responsive hydrogel based on NIPAAm. Li et al. demonstrated the effectiveness of a composite hydrogel, incorporating NIPAAm and Dox, previously applied in N−P hydrogel, for the treatment of choroidal melanoma in a nude mouse tumor model.[35] Furthermore, Zhang et al. have substantiated the effectiveness of a multifunctional nanocarrier, targeting herceptin-positive breast cancer, which is developed with in situ loading of DOX and includes NIPAAm-based nanogels, through in vivo models.[36] Additionally, Zhao et al. indicated the potential for tumor phototherapy using programmed stimuli-responsive hybrid nanogels with NIPAAm in a mouse *in vivo* model.[37] While the current results provide promising indications, further research must address these critical issues to advance the N−P hydrogel toward potential clinical translation. Comprehensive *in vivo* studies will not only shed light on the performance of N−P hydrogel in a more realistic setting but also ensure its safe and effective use in patients, ultimately paving the way for innovative and impactful advancements in cancer treatment and regenerative medicine.

4. CONCLUSIONS

In this study, we successfully developed a functional N−P hydrogel incorporating PVA into NIPAAm. The N−P hydrogel exhibited excellent temperature-responsive behavior with an LCST at around 34 °C, which is suitable for biomedical applications. The presence of PVA in the hydrogel contributed to increased porosity and rapid drug release behavior, especially in the N−P3 group. The N−P hydrogel demonstrated controlled drug release, biocompatibility, and potential for effective anticancer drug delivery in melanoma cells. In conclusion, the N−P hydrogel system presents a promising platform for controlled drug delivery and anticancer applications. Its ability to exhibit temperature-responsive behavior, rapid drug release, and biocompatibility holds great potential for various biomedical applications including skin regeneration and cancer treatment. Further research, including in vivo studies, will be pivotal in advancing the N−P hydrogel system toward clinical translation and opening new avenues for innovative and impactful advancements in the field of regenerative medicine and cancer therapeutics.

AUTHOR INFORMATION

Corresponding Authors

Dong Nyoung Heo − *Biofirends Inc., Seoul 02447, Republic of Korea; Department of Dental Materials, School of Dentistry, Kyung Hee University, Seoul 02447, Republic of Korea;* orcid.org/0000-0002-7717-7184; Email: heodaeng@khu.ac.kr

Il Keun Kwon − *Department of Dental Materials, School of Dentistry, Kyung Hee University, Seoul 02447, Republic of Korea; Kyung Hee University Medical Science Research Institute, Kyung Hee University, Seoul 02447, Republic of Korea;* orcid.org/0000-0001-9649-3003; Email: kwoni@khu.ac.kr

Authors

Jae Hwan Choi − *Department of Biomedical Science and Technology, Graduate School, Kyung Hee University, Seoul 02447, Republic of Korea; Biofirends Inc., Seoul 02447, Republic of Korea*

Jae Seo Lee − *Department of Dental Materials, School of Dentistry, Kyung Hee University, Seoul 02447, Republic of Korea; Division of Engineering in Medicine, Brigham and Women's Hospital, Harvard Medical School, Cambridge, Massachusetts 02139, United States*

Dae Hyeok Yang − *Institute of Cell and Tissue Engineering, College of Medicine, The Catholic University of Korea, Seoul 06591, Republic of Korea*

Haram Nah − *Biofirends Inc., Seoul 02447, Republic of Korea; Department of Dentistry, Graduate School, Kyung Hee University, Seoul 02447, Republic of Korea*

Sung Jun Min − *Department of Dentistry, Graduate School, Kyung Hee University, Seoul 02447, Republic of Korea*

Seung Yeon Lee − *Department of Dentistry, Graduate School, Kyung Hee University, Seoul 02447, Republic of Korea*

Ji Hye Yoo − *Department of Biomedical Science and Technology, Graduate School, Kyung Hee University, Seoul 02447, Republic of Korea*

Heung Jae Chun − *Institute of Cell and Tissue Engineering, College of Medicine, The Catholic University of Korea, Seoul 06591, Republic of Korea*

Ho-Jin Moon − *Department of Dental Materials, School of Dentistry, Kyung Hee University, Seoul 02447, Republic of Korea*

Young Ki Hong − *Department of Biomedical Materials, Konyang University, Daejeon 35365, Republic of Korea*

Complete contact information is available at: https://pubs.acs.org/10.1021/acsomega.3c06291

Author Contributions

◆J.H.C., J.S.L., and D.H.Y. contributed equally to this work.

Notes

The authors declare no competing financial interest.

ACKNOWLEDGMENTS

This work was supported by the National Research Foundation of Korea (NRF) grant funded by the Korea Government (MSIT) (NRF-2020R1A2C2011937), a grant of the Korea Health Technology R&D Project through the Korea Health Industry Development Institute (KHIDI) funded by the Ministry of Health & Welfare (HI22C1572), and the Ministry of Trade, Industry & Energy (MOTIE, Republic of Korea; Grant No. 20017645).

REFERENCES

(1) Gordon, R. Skin cancer: an overview of epidemiology and risk factors. *Semin. Oncol. Nurs.* **2013**, *29* (3), 160−169. Hayward, N. K.; Wilmott, J. S.; Waddell, N.; Johansson, P. A.; Field, M. A.; Nones, K.; Patch, A. M.; Kakavand, H.; Alexandrov, L. B.; Burke, H.; et al. Whole-genome landscapes of major melanoma subtypes. *Nature* **2017**, *545* (7653), 175−180. Ossio, R.; Roldan-Marin, R.; Martinez-Said, H.; Adams, D. J.; Robles-Espinoza, C. D. Melanoma: a global perspective. *Nat. Rev. Cancer* **2017**, *17* (7), 393−394.

(2) Liu, Y.; Sheikh, M. S. Melanoma: molecular pathogenesis and therapeutic management. *Mol. Cell. Pharmacol.* **2014**, *6* (3), 228.

(3) Capanema, N. S. V.; Carvalho, I. C.; Mansur, A. A. P.; Carvalho, S. M.; Lage, A. P.; Mansur, H. S. Hybrid Hydrogel Composed of Carboxymethylcellulose−Silver Nanoparticles−Doxorubicin for Anti-cancer and Antibacterial Therapies against Melanoma Skin Cancer Cells. *ACS Appl. Nano Mater.* **2019**, *2* (11), 7393−7408.

(4) Cassano, R.; Cuconato, M.; Calviello, G.; Serini, S.; Trombino, S. Recent Advances in Nanotechnology for the Treatment of Melanoma. *Molecules* **2021**, *26* (4), No. 785, DOI: 10.3390/molecules26040785. Jiang, B. P.; Zhang, L.; Guo, X. L.; Shen, X.

C.; Wang, Y.; Zhu, Y.; Liang, H. Poly(N-phenylglycine)-Based Nanoparticles as Highly Effective and Targeted Near-Infrared Photothermal Therapy/Photodynamic Therapeutic Agents for Malignant Melanoma. *Small* **2017**, *13* (8), No. 1602496, DOI: 10.1002/smll.201602496.

(5) Svedman, F. C.; Spanopoulos, D.; Taylor, A.; Amelio, J.; Hansson, J. Surgical outcomes in patients with cutaneous malignant melanoma in Europe - a systematic literature review. *J. Eur. Acad. Dermatol. Venereol.* **2017**, *31* (4), 603−615.

(6) Askari, E.; Naghib, S. M.; Zahedi, A.; Seyfoori, A.; Zare, Y.; Rhee, K. Y. Local delivery of chemotherapeutic agent in tissue engineering based on gelatin/graphene hydrogel. *J. Mater. Res. Technol.* **2021**, *12*, 412−422. Tang, X.; Chen, X.; Zhang, S.; Gu, X.; Wu, R.; Huang, T.; Zhou, Z.; Sun, C.; Ling, J.; Liu, M.; Yang, Y. Silk-Inspired In Situ Hydrogel with Anti-Tumor Immunity Enhanced Photodynamic Therapy for Melanoma and Infected Wound Healing. *Adv. Funct. Mater.* **2021**, *31* (17), No. 2101320, DOI: 10.1002/adfm.202101320. He, D.; Li, H. Bifunctional Cx43 Mimic Peptide Grafted Hyaluronic Acid Hydrogels Inhibited Tumor Recurrence and Stimulated Wound Healing for Postsurgical Tumor Treatment. *Adv. Funct. Mater.* **2020**, *30* (51), No. 2004709, DOI: 10.1002/adfm.202004709.

(7) Nardin, C.; Schlaad, H. *Biological Soft Matter*; Wiley Online Library, 2021. Hennink, W. E.; van Nostrum, C. F. Novel crosslinking methods to design hydrogels. *Adv. Drug Delivery Rev.* **2012**, *64*, 223−236. Min, S. J.; Lee, J. S.; Nah, H.; Moon, H.-J.; Lee, S. J.; Kang, H. J.; Hwang, Y.-S.; Kwon, I. K.; Heo, D. N. Degradable and Tunable Keratin-fibrinogen Hydrogel as Controlled Release System for Skin Tissue Regeneration. *J. Bionic Eng.* **2023**, *20* (3), 1049−1059. Khadivar, P.; Khajeniazi, S.; Karimi, A. Preparation of a carboxymethylated diethyl aminoethyl cellulose-collagen nanocomposite scaffold as a candidate for skin tissue engineering. *J. Mater. Res. Technol.* **2022**, *19*, 3966−3979.

(8) Gutowska, A.; Bark, J. S.; Kwon, I. C.; Bae, Y. H.; Cha, Y.; Kim, S. W. Squeezing hydrogels for controlled oral drug delivery. *J. Controlled Release* **1997**, *48* (2−3), 141−148. Sun, L.-F.; Zhuo, R.-X.; Liu, Z.-L. Studies on the Synthesis and Properties of Temperature Responsive and Biodegradable Hydrogels. *Macromol. Biosci.* **2003**, *3* (12), 725−728.

(9) Das, D.; Ghosh, P.; Ghosh, A.; Haldar, C.; Dhara, S.; Panda, A. B.; Pal, S. Stimulus-Responsive, Biodegradable, Biocompatible, Covalently Cross-Linked Hydrogel Based on Dextrin and Poly(N-isopropylacrylamide) for in Vitro/in Vivo Controlled Drug Release. *ACS Appl. Mater. Interfaces* **2015**, *7* (26), 14338−14351. Lu, N.; Yang, K.; Li, J.; Weng, Y.; Yuan, B.; Ma, Y. Controlled drug loading and release of a stimuli-responsive lipogel consisting of poly(N-isopropylacrylamide) particles and lipids. *J. Phys. Chem. B* **2013**, *117* (33), 9677−9682.

(10) Schild, H. G. Poly (N-isopropylacrylamide): experiment, theory and application. *Prog. Polym. Sci.* **1992**, *17* (2), 163−249. Gil, E.; Hudson, S. Stimuli-reponsive polymers and their bioconjugates. *Prog. Polym. Sci.* **2004**, *29* (12), 1173−1222. Bromberg, L. E.; Ron, E. S. Temperature-responsive gels and thermogelling polymer matrices for protein and peptide delivery. *Adv. Drug Delivery Rev.* **1998**, *31* (3), 197−221. Burek, M.; Kowalczyk, M.; Czuba, Z. P.; Krol, W.; Pilawka, R.; Waskiewicz, S. Poly(N-isopropylacrylamide) hydrogels cross-linked by α,α-trehalose diacetals as thermo-responsive and acid-degradable carriers for drug delivery. *Polym. Degrad. Stab.* **2016**, *129*, 296−305. Banerjee, I.; Mishra, D.; Das, T.; Maiti, T. K. Wound pH-responsive sustained release of therapeutics from a poly(NIPAAm-co-AAc) hydrogel. *J. Biomater. Sci., Polym. Ed.* **2012**, *23* (1−4), 111−132.

(11) Constantin, M.; Bucatariu, S.; Harabagiu, V.; Popescu, I.; Ascenzi, P.; Fundueanu, G. Poly(N-isopropylacrylamide-co-methacrylic acid) pH/thermo-responsive porous hydrogels as self-regulated drug delivery system. *Eur. J. Pharm. Sci.* **2014**, *62*, 86−95.

(12) Zhang, J. T.; Huang, S. W.; Cheng, S. X.; Zhuo, R. X. Preparation and properties of poly (N-isopropylacrylamide)/poly (N-isopropylacrylamide) interpenetrating polymer networks for drug delivery. *J. Polym. Sci., Part A: Polym. Chem.* **2004**, *42* (5), 1249−1254.

(13) Alvarez-Lorenzo, C.; Concheiro, A.; Dubovik, A. S.; Grinberg, N. V.; Burova, T. V.; Grinberg, V. Y. Temperature-sensitive chitosan-poly(N-isopropylacrylamide) interpenetrated networks with enhanced loading capacity and controlled release properties. *J. Controlled Release* **2005**, *102* (3), 629−641.

(14) Li, B.; Jiang, Y.; Liu, Y.; Wu, Y.; Yu, H.; Zhu, M. Novel poly(N-isopropylacrylamide)/clay/poly(acrylamide) IPN hydrogels with the response rate and drug release controlled by clay content. *J. Polym. Sci., Part B: Polym. Phys.* **2009**, *47* (1), 96−106, DOI: 10.1002/polb.21618.

(15) Gil, E. S.; Hudson, S. M. Effect of silk fibroin interpenetrating networks on swelling/deswelling kinetics and rheological properties of poly (N-isopropylacrylamide) hydrogels. *Biomacromolecules* **2007**, *8* (1), 258−264.

(16) Dragan, E. S. Design and applications of Interpenetrating polymer networks: an overview. *Chem. Eng. J.* **2014**, *243*, 572−590.

(17) Jiang, S.; Liu, S.; Feng, W. PVA hydrogel properties for biomedical application. *J. Mech. Behav. Biomed. Mater.* **2011**, *4* (7), 1228−1233.

(18) Wenceslau, A. C.; dos Santos, F. G.; Ramos, É. R. F.; Nakamura, C. V.; Rubira, A. F.; Muniz, E. C. Thermo- and pH-sensitive IPN hydrogels based on PNIPAAm. and PVA-Ma networks with LCST tailored close to human body temperature. *Mater. Sci. Eng. C* **2012**, *32* (5), 1259−1265.

(19) Zhang, J. T.; Bhat, R.; Jandt, K. D. Temperature-sensitive PVA/PNIPAAm semi-IPN hydrogels with enhanced responsive properties. *Acta Biomater.* **2009**, *5* (1), 488−497.

(20) Reddy, L. H.; Murthy, R. Pharmacokinetics and biodistribution studies of doxorubicin loaded poly (butyl cyanoacrylate) nanoparticles synthesized by two different techniques. *Biomed. Pap. Med. Fac. Univ Palacky* **2004**, *148* (2), 161−166. Di Martino, A.; Kucharczyk, P.; Capakova, Z.; Humpolicek, P.; Sedlarik, V. Chitosan-based nanocomplexes for simultaneous loading, burst reduction and controlled release of doxorubicin and 5-fluorouracil. *Int. J. Biol. Macromol.* **2017**, *102*, 613−624.

(21) Zhang, X.-Z.; Chu, C.-C. Synthesis and properties of the semi-interpenetrating polymer network-like, thermosensitive poly(N-isopropylacrylamide) hydrogel. *J. Appl. Polym. Sci.* **2003**, *89* (7), 1935−1941.

(22) Gao, Y.; Chen, X.; Liao, B.; Ding, X.; Zheng, Z.; Cheng, X.; Pang, H.; Peng, Y. Polyelectrolyte Self-assembly Approach to Smart Nanocontainers. *Polym. Bull.* **2006**, *56* (4−5), 305−311.

(23) Gong, Y.; Liu, Q. L.; Zhu, A. M.; Zhang, Q. G. One-pot synthesis of poly(N-isopropylacrylamide)/chitosan composite microspheres via microemulsion. *Carbohydr. Polym.* **2012**, *90* (1), 690−695.

(24) Güngör, A.; Demir, D.; Bölgen, N.; Özdemir, T.; Genç, R. Dual stimuli-responsive chitosan grafted poly(NIPAM-co-AAc)/poly(vinyl alcohol) hydrogels for drug delivery applications. *Int. J. Polym. Mater. Polym. Biomater.* **2021**, *70* (11), 810−819.

(25) Mansur, H. S.; Sadahira, C. M.; Souza, A. N.; Mansur, A. A. P. FTIR spectroscopy characterization of poly (vinyl alcohol) hydrogel with different hydrolysis degree and chemically crosslinked with glutaraldehyde. *Mater. Sci. Eng. C* **2008**, *28* (4), 539−548.

(26) Kaneko, Y.; Yoshida, R.; Sakai, K.; Sakurai, Y.; Okano, T. Temperature-responsive shrinking kinetics of poly (N-isopropylacrylamide) copolymer gels with hydrophilic and hydrophobic comonomers. *J. Membr. Sci.* **1995**, *101* (1−2), 13−22.

(27) Zhang, J.-T.; Cheng, S.-X.; Huang, S.-W.; Zhuo, R.-X. Temperature-Sensitive Poly(N-isopropylacrylamide) Hydrogels with Macroporous Structure and Fast Response Rate. *Macromol. Rapid Commun.* **2003**, *24* (7), 447−451.

(28) Zhang, J.-T.; Cheng, S.-X.; Zhuo, R.-X. Poly(vinyl alcohol)/poly(N-isopropylacrylamide) semi-interpenetrating polymer network hydrogels with rapid response to temperature changes. *Colloid Polym. Sci.* **2003**, *281* (6), 580−583.

(29) Li, Z.; Bai, H.; Zhang, S.; Wang, W.; Ma, P.; Dong, W. DN strategy constructed photo-crosslinked PVA/CNC/P(NIPPAm-co-AA) hydrogels with temperature-sensitive and pH-sensitive properties. *New J. Chem.* **2018**, *42* (16), 13453−13460.

(30) Oveissi, F.; Spinks, G. M.; Naficy, S. Bond Reformation, Self-Recovery, and Toughness in Hydrogen-Bonded Hydrogels. *ACS Appl. Polym. Mater.* **2020**, *2* (12), 5798−5807. Song, P.; Xu, Z.; Guo, Q. Bioinspired Strategy to Reinforce PVA with Improved Toughness and Thermal Properties via Hydrogen-Bond Self-Assembly. *ACS Macro Lett.* **2013**, *2* (12), 1100−1104. Bi, S.; Pang, J.; Huang, L.; Sun, M.; Cheng, X.; Chen, X. The toughness chitosan-PVA double network hydrogel based on alkali solution system and hydrogen bonding for tissue engineering applications. *Int. J. Biol. Macromol.* **2020**, *146*, 99−109.

(31) Koehler, J.; Brandl, F. P.; Goepferich, A. M. Hydrogel wound dressings for bioactive treatment of acute and chronic wounds. *Eur. Polym. J.* **2018**, *100*, 1−11.

(32) Kumashiro, Y.; Lee, W. K.; Ooya, T.; Yui, N. Enzymatic Degradation of Semi-IPN Hydrogels Based on N-Isopropylacrylamide and Dextran at a Specific Temperature Range. *Macromol. Rapid Commun.* **2002**, *23* (7), 407 DOI: 10.1002/1521-3927(20020401)23:7<407::AID-MARC407>3.0.CO;2-7.

(33) Santos, J. R.; Alves, N. M.; Mano, J. F. New Thermo-responsive Hydrogels Based on Poly (N-isopropylacrylamide)/ Hyaluronic Acid Semi-interpenetrated Polymer Networks: Swelling Properties and Drug Release Studies. *J. Bioact. Compat. Polym.* **2010**, *25* (2), 169−184.

(34) Oliveira, K. B.; Palú, É.; Weffort-Santos, A. M.; Oliveira, B. H. Influence of rosmarinic acid and Salvia officinalis extracts on melanogenesis of B16F10 cells. *Rev. Bras. Farmacogn.* **2013**, *23* (2), 249−258. Gismondi, A.; Nanni, V.; Reina, G.; Orlanducci, S.; Terranova, M. L.; Canini, A. Nanodiamonds coupled with 5,7-dimethoxycoumarin, a plant bioactive metabolite, interfere with the mitotic process in B16F10 cells altering the actin organization. *Int. J. Nanomed.* **2016**, *11*, 557−574.

(35) Li, L.; Zeng, Z.; Chen, Z.; Gao, R.; Pan, L.; Deng, J.; Ye, X.; Zhang, J.; Zhang, S.; Mei, C.; et al. Microenvironment-Triggered Degradable Hydrogel for Imaging Diagnosis and Combined Treatment of Intraocular Choroidal Melanoma. *ACS Nano* **2020**, *14* (11), 15403−15416.

(36) Zhang, X.; Wei, P.; Wang, Z.; Zhao, Y.; Xiao, W.; Bian, Y.; Liang, D.; Lin, Q.; Song, W.; Jiang, W.; Wang, H. Herceptin-Conjugated DOX-Fe(3)O(4)/P(NIPAM-AA-MAPEG) Nanogel System for HER2-Targeted Breast Cancer Treatment and Magnetic Resonance Imaging. *ACS Appl. Mater. Interfaces* **2022**, *14* (14), 15956−15969.

(37) Zhao, C.; Sun, S.; Li, S.; Lv, A.; Chen, Q.; Jiang, K.; Jiang, Z.; Li, Z.; Wu, A.; Lin, H. Programmed Stimuli-Responsive Carbon Dot-Nanogel Hybrids for Imaging-Guided Enhanced Tumor Phototherapy. *ACS Appl. Mater. Interfaces* **2022**, *14* (8), 10142−10153.

https://doi.org/10.1021/acsomega.3c06291
ACS Omega 2023, 8, 44076−44085